Development of a nano-heat transfer fluid carrying direct absorbing receiver for concentrating solar collectors

Ashley Toppin-Hector and Harjit Singh*
School of Engineering and Design, Brunel University, Uxbridge, Middlesex UB8 3PH, UK

Abstract

A MATLAB-based computer model to design a novel directly absorbing receiver system (DARS) for concentrating solar collectors employing nanofluid-based solar radiation volumetric absorption is presented. Graphene and aluminum nanosphere-based suspensions in Therminol VP-1 were simulated to identify the optimum thermo-geometric configuration of a DARS comprising a transparent all glass tubular absorber. Several particle concentrations were simulated scrutinizing the optical response of the two colloidal dispersions to yield a minimum supply temperature of 250°C; further investigated are the implications of fluid flow velocity upon system yield. The resulting temperature fields and geometric dimensions of the DARS are predicted. Findings demonstrate that the DARS is able to deliver heat at ∼265°C with a receiver tube diameter of 5 mm opposed to commercially available 70-mm diameter metallic absorbers.

Keywords: concentrating solar collector; graphene nanoparticles; aluminium nanoparticles; nano-heat transfer fluid; direct absorption

*Corresponding author.
harjit.singh@brunel.ac.uk

Received 5 July 2013; revised 5 September 2013; accepted 6 September 2013

1 INTRODUCTION

If the ambitious long-term goals of the EU for the fraction of total energy supply from renewable sources are to be achieved, it is essential that, in addition to electricity generation and transport, heat is also considered. Many industrial and commercial processes require heat in the range between 80 and 250°C. The potential for new designs of compact solar energy collectors operating in the medium temperature range, which achieve higher conversion efficiencies than current devices in a cost-effective manner, is thus very high. Flat plate solar collectors and parabolic trough collectors (PTCs), with an aperture width of ∼4–6 m, for, respectively, supplying heat at temperatures <80°C and ∼390°C are commercially available. The current class of PTCs employs selectively coated steel absorber tubes, which are susceptible to degradation on sustained exposure to heat and vacuum loss as a result of fractures formed in the outer glass tube due to the existence of residual thermal stresses induced in the glass-to-metal seal upon manufacture [1]. The installed cost of PTCs is also very high, €250–350/m^2 [2]. The development of solar collectors for medium temperature range applications to supply heat at temperatures of 250°C and above, with high efficiency >50%, requires either improvements in the performance of the systems adapted from current designs achieved by improving the optics and reducing the heat loss or the development of new families of collectors with bespoke optical performance and refined innovation to inhibit thermal losses.

Advances in nanotechnology to date give rise to pivotal concepts regarding synthesis of a new class of engineering fluids via the application of nanomaterials to conventional heat transfer fluids, elaborating on many basic theories and early attempts by past pioneers such as Abdelrahman *et al.* [3] who explored the feasibility of direct solar thermal absorption using particle-laden gases. This paper explores the prospect of using a DARS introducing a paradigm shift concerning solar energy absorption mechanisms exhibited by employing conceptual nanofluids of Therminol VP-1 with trace amounts of dispersed graphene and aluminium in conjunction with concentrating solar collectors for supplying heat at the prescribed benchmark of 250°C. To suppress convective heat loss, the receiver was enclosed within an evacuated glass envelope [4]. Heat transfer to the nanofluid (working fluid) is approximated as coupled radiative and conduction heat transfer in the absorbing, emitting and scattering medium.

International Journal of Low-Carbon Technologies 2016, 11, 199–204

doi:10.1093/ijlct/ctt072 Advance Access Publication 10 October 2013

A MATLAB-based computer model was developed to simulate several particle concentrations of graphene and aluminium nanosphere-based suspensions in Therminol VP-1 scrutinizing the thermo-fluidic and optical response of the two colloidal dispersions to yield the aforementioned benchmark mean fluid supply temperature of 250°C. The resulting temperature fields and optimum configuration of DARS are presented. Further explored are the implications of fluid flow velocity upon system output.

2 THEORETICAL MODEL

A DARS receiver differs from a conventional solar PTC receiver on the merit that the metal absorber tube is replaced by a glass tube allowing the working fluid traversing the receiver to directly interact with incident solar irradiance. Volumetric energy absorption is displayed, characteristically enhanced via absorption and scattering mechanisms intrinsic to suspended nanoparticles within the working fluid.

Numerical finite-difference schemes were employed in the MATLAB model to predict the thermo-fluidic characteristics of nano-heat transfer fluids, model their optical response and resolve the resultant temperature field exhibited. A section view along the length of the DARS has been modeled by discretizing the entire participating medium into a rectangular Cartesian finite-difference grid, see Figure 1.

The values of the thermo-physical properties used for the nanomaterials and base fluid to facilitate theoretical synthesis of the nanofluids are given in Table 1; the data reported were gathered from external resources [5–7].

Thermo-physical properties of the nanomaterials are expected to vary from that of the bulk at nanoscale. However, upon dispersing these nanomaterials within the medium, such properties may also exhibit further changes. This is due to interfacial interactions between neighboring nanoparticles that are heavily influenced by the directional orientation as well as the spatial distribution of the nanomaterials within the medium [7]. For simplicity, in this study, the thermo-physical properties have been assumed to remain the same as bulk.

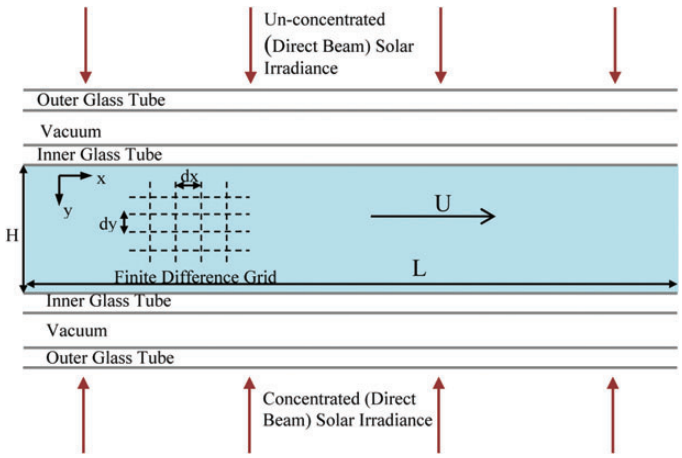

Figure 1. *Section view of the DARS.*

The effective density and specific heat of the nanofluid are computed by applying the parallel mixture rule shown in the following equation [8]:

$$X_{nf} = f_v X_{np} + (1 - f_v) X_f \tag{1}$$

where f_v is the volume fraction of the dispersed phase and X is the thermo-physical property such as density or specific heat.

The effective thermal conductivity of the nanofluid has been computed using the modified Maxwell model given by the following equation [9]:

$$k_{nf} = \frac{k_{cp} + 2k_f + 2(k_{cp} - k_f)(1 - \beta)^3 f_v}{k_{cp} + 2k_f - (k_{cp} - k_f)(1 + \beta)^3 f_v} k_f \tag{2}$$

where β is the ratio between interfacial layer thickness and spherical radius, k_{nf} is the effective thermal conductivity of the nanofluid, k_f is the thermal conductivity of the base fluid and k_{cp} is the thermal conductivity of the complex particle computed using formulations derived in the work of Yu and Choi [9]. A complex particle is a three-phase representation consisting of the nanoparticles, the interfacial layer; an ordered agglomeration of liquid particles at the liquid–solid interface, and the surrounding base fluid medium this representation was postulated by Leong *et al.* [10].

The spectral normal direct beam irradiance data in Jodhphur, Rajasthan, India, were extracted from the SMARTS model [11, 12]. The longitude, latitude, date and time are among some of the user inputs specified in the SMARTS model to ascertain the global location whilst mapping the solar position to yield accurate solar irradiance data for use in the mathematical model. The SMARTS model yielded a direct normal beam irradiance of 650 W m^{-2}.

The spectral range considered in the current analysis was truncated to encompass radiation within the visible range in the wavelength band between 0.28 and 0.86 μm. Thermal re-emission from the participating media in the form of long-wave radiation of spectral wavelengths $\lambda > 0.86$ μm; from both the nanoparticles and base fluid have not been factored into this analysis. Attenuation of radiation corresponds to the energy gained by the medium and has been quantified using Lambert–

Table 1. *Thermo-physical properties of nanomaterials and base fluid.*

	Graphene	Aluminum	Therminol VP-1
Density (kg m^{-3})	1000	2700	1060
Thermal conductivity (W m^{-1} K^{-1})	5000	247	0.1357
Specific heat (J kg^{-1} K^{-1})	1250	900	1570

Beer's law mathematically given by the following equation [13]:

$$\frac{\partial I_\lambda}{\partial y} = -(K_{af\lambda} + K_{enp\lambda})I_\lambda = -K_{enf\lambda}I_\lambda \tag{3}$$

where $K_{af\lambda}$ is the spectral absorption coefficient for the base fluid, $K_{enp\lambda}$ is the spectral extinction coefficient for the nanoparticle and $K_{enf\lambda}$ is the spectral extinction coefficient for the nanofluid and I_λ is the spectral intensity of solar radiation measured in $W\,m^{-2}$. For pure fluids, scattering due to the fluid can be neglected; hence, radiant intensity attenuation due to the base fluid caused by absorption only is required for consideration. As independent scattering of the spectral quantities was assumed; an assumption valid for low volume fractions of nanomaterials, the extinction coefficient for the nanofluid was approximated as a coupled effect due to absorption by the base fluid and combined absorption and scattering by the nanoparticles superimposing the two quantities via addition. The spectral absorption coefficient for the base fluid was computed using the following equation [13]:

$$K_{af\lambda} = \frac{4\pi\kappa}{\lambda} \tag{4}$$

where κ is the index of absorption and λ is the wavelength of the incident radiation.

The absorption index varies with wavelength; values for κ in the spectral range considered have been taken from Taylor *et al.* [14] and Otanicar *et al.* [15]. The spectral extinction coefficient for the nanoparticle was given by the mathematical expression shown in the following equation [14]:

$$K_{enp\lambda} = \frac{3f_v Q_{enp\lambda}(\alpha, m)}{2D} \tag{5}$$

where $Q_{enp\lambda}$ is the extinction efficiency yielded via implementation of Rayleigh's regimes, which entails evaluation of complex algebraic functions for absorption and scattering of radiations, details of these expression can be found elsewhere [16], α is the size parameter, m is the relative complex refractive index, computed using the complex refractive index of the nanoparticles encompassing the imaginary component such that ($m_{particle} = n + i\kappa$) together with the refractive index of the base fluid (n_{fluid}) in accordance with the following equation [13]:

$$m = \frac{m_{particle}}{n_{fluid}} \tag{6}$$

Such that the relative complex refractive index is given by ($m = n + i\kappa$) and D is the spherical diameter of the nanoparticle. In this instance, the graphene and aluminium particles had a fixed spherical diameter of 5 nm.

The heat transfer model employed was a two-dimensional steady-state analysis given by Equation (7). The energy balance equation was solved at each node using explicit central finite-difference approximations for the first- and second-derivative terms. In this case, heat transfer entailed primarily, radiative heat exchange between the sun and the participating medium, thermal conduction between fluid elements within the medium, and combined radiative and convective heat exchange at the system boundaries to the sky and to the ambient surroundings, respectively. On the nanometric scale, it is inferred that the particles directly absorb radiation incident upon them and elevate in temperature, consequently heat is transferred from the suspended particles to surrounding fluid elements via thermal conduction and convection. Radiative heat exchange from the particles to the surrounding fluid elements is in the form of long-wave radiation. Long-wave radiation has been omitted as a potential energy source by truncating the spectral range, as such radiative heat exchange from the particles to the fluid elements has been omitted also.

$$k\frac{\partial^2 T}{\partial x^2} + k\frac{\partial^2 T}{\partial y^2} - \frac{\partial q_r}{\partial y} = \rho C_p U\frac{\partial T}{\partial x} \tag{7}$$

where k, ρ, C_p are, respectively, the thermal conductivity, the density and the specific heat of the nanofluid, U is the axial fluid velocity, q_r is the solar radiant heat flux and T is the fluid temperature.

2.1 Modeling parameters

To facilitate computation of Lambert–Beer's Equation (3), and the energy balance Equation (7), finite-difference techniques were employed. As such the spectral and spatial domains were divided into uniform nodes of finite differences as conveyed by Figure 1, to warrant discretization of the aforementioned governing equations. The DARS has an inner diameter (H) of 0.005 m (5 mm), this was divided into 201 nodes, corresponding to 200 finite differences, with each cell having a thickness of 0.000025 m. The length (L) of the DARS was 56.84 m, which was divided into 28 421 nodes, corresponding to 28 420 finite differences, with each cell having a length of 0.002 m. The following dimensions correspond to 14 DARS; each 4.06 m long aligned in series. The spectral domain in the wavelength range between 0.28 and 0.86 μm was also divided into 29 uniform bands each with a width of 0.02 μm. For continuity upon resizing of the DARS diameter, the step size along the y-axis was conserved at 0.000025 m. Lambert–Beer's law was computed using a first-order backward difference discretization whilst the energy balance equation was solved using first-order central difference discretization. In both instances, the equations were solved explicitly at each node.

Initially, the fluid in the DARS is assumed to be at a uniform temperature of 35°C. Similarly, the temperature of the fluid entering the DARS is constant at a fixed temperature of 35°C. The iterations proceed until the working fluid has traversed the entire length of the DARS. The boundary condition applied along the length of the DARS at the top and bottom surfaces of the outer glass tube, see Figure 1, is of a combined convective and radiative nature shown in Equation (8). This quantifies the total heat loss, $q_{l,}$ incorporating constant convective and

radiative heat transfer losses from the DARS to the surroundings and to the sky, respectively.

$$q_l = q_{\text{conv}} + q_{\text{rad}} = h_{\text{ann}}(T - T_{\text{amb}}) + \varepsilon\sigma(T_{\text{gt}}^4 - T_{\text{sky}}^4) \qquad (8)$$

The convective component, q_{conv}, of the total heat loss is heavily dominated by the heat transfer characteristics of the annulus region. The convective heat transfer coefficient, h_{ann}, in the annulus, an evacuated region filled with low pressure air, is 0.000115 W m^{-2} K^{-1}. The temperature of the ambient air, T_{amb}, is 30°C. The radiative component of the total heat loss is denoted by q_{rad}. As the glass temperature, T_{gt}, elevates, there is radiative exchange to the sky held at 21°C, the sky temperature T_{sky}. The emissivity ε of the glass is 0.95 and σ is the Stefan–Boltzmann constant valued at 5.6704 × 10^{-8} W m^{-2} K^{-4}.

3 RESULTS AND DISCUSSION

Spectral extinction coefficients of graphene–Therminol VP-1 and aluminium–Therminol VP-1 nanofluids were predicted, Figure 2, for a range of volume fractions and compared with those published by other researchers [14, 15] for the base fluid Therminol VP-1 alone.

Clearly, addition of nanomaterials to Therminol VP-1 significantly increased the extinction capability of the working fluid resulting into an enhanced solar-weighted absorption relative to that of Therminol VP-1 alone. It can be seen from Figure 2 that graphene nanoparticles exhibited higher solar absorption capabilities, relative to aluminium nanoparticles, causing radiant intensity attenuation within the medium at a quicker rate per unit depth at the same volume fraction; this is reflected by the fact that the extinction coefficients in the graphene–Therminol VP-1 are larger relative to the aluminium–Therminol VP-1 nanofluid at any given particle concentration.

However, in direct absorption solar thermal energy system, an accelerated rate of extinction is not necessarily the only characteristic sought as particular consideration must be given to selecting a volume fraction of nanoparticles that will result into highest average nanofluid outlet temperature relative to the diameter of the receiver tube. As conveyed by Figure 2, an increase in the spectral extinction coefficients is exhibited as the particle volume fraction is increased. Spectral extinction coefficients have direct implications upon the radiant intensity attenuation rate within the medium consequently augmenting the temperature distribution within the DARS.

High particle volume fractions act to increase spectral extinction coefficients; consequently, the DARS then begins to resemble a conventional surface-based absorber; in these instances, large amounts of incident radiations are absorbed by fluid elements near the system boundaries with little or no heat flux permeating to fluid layers deeper within the DARS away from the boundaries. Fluid elements in these boundary regions elevate significantly in temperature, subsequently heat is transmitted further throughout the medium via thermal conduction as opposed to gaining heat via direct absorption. Due to the inherently poor thermal conductivity of the working fluid, there are large regions present within the DARS where fluid temperature is invariant from the inlet temperature, ultimately the mean fluid outlet temperature delivered reduces, reflecting a negative impact upon thermal efficiency of the DARS. Conversely, if the particle volume fraction is too low, optical efficiency is severely reduced as the working fluid no longer captures all of the solar radiant flux; low particle volume fractions yield a medium with low optical thickness, thus a greater depth of fluid would be required to capture all radiations incident. In this instance, the mean fluid outlet temperature suffers due to poor solar absorption capabilities. The optimum particle volume fraction must be ascertained to maximize the system output. Within the computational limits (i.e. DARS diameter, particle size, concentration ratio etc.) explored in this paper, the optimum particle volume fractions were 0.02 and 0.09% for graphene and aluminum nanoparticles, respectively.

Simulations showed that volume fractions of 0.02% of graphene and 0.09% of aluminum nanoparticles achieved almost similar extinction coefficients resulting into similar mean fluid temperatures as shown in Figure 3; when the DARS diameter

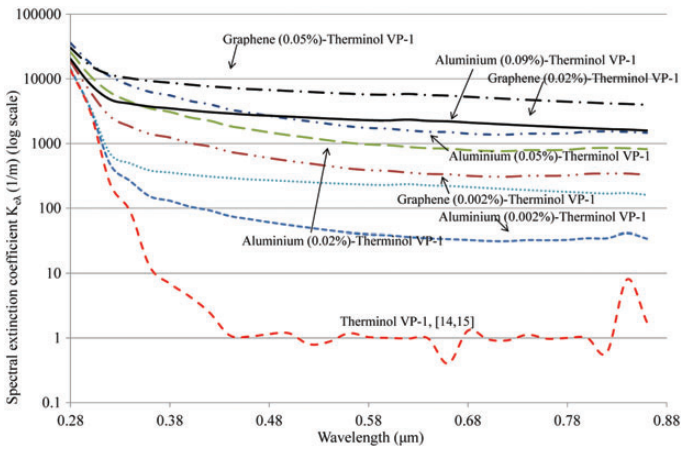

Figure 2. *Spectral extinction coefficients of graphene and aluminum nanofluids.*

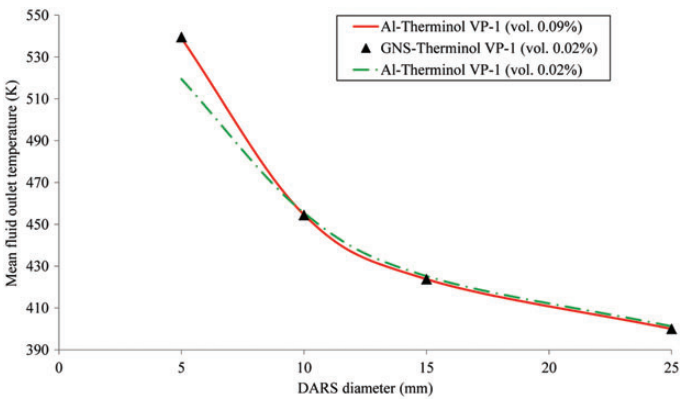

Figure 3. *Mean nanofluid outlet temperatures for a range of DARS diameters.*

was varied from 5 to 25 mm. These simulations assumed a solar concentrator with a concentration ratio of 40, which means a total incident irradiance of 26 000 W m^{-2} on the receiver based on an irradiance of 650 W m^{-2} received on the collector aperture.

Thermal conductivity, specific heat and density of Therminol VP-1 varied negligibly upon addition of graphene or aluminum nanoparticles due to the small volume fractions studied. The thermo-physical property determination formulations incorporated within the model are of a semi-empirical nature. Such formulations undergo continual review and often developments are made subsequently via revision of the mathematical expressions or addition of further parameters theorized to be influential. Due to this, further work should always aspire to adopt the most current formulations acquiring further parameters, if necessary, to ascertain the thermo-physical property enhancements that can be achieved from suspension of nanomaterials within heat transfer fluids.

It can be seen from Figure 3 that the outlet temperature increased as the DARS diameter was reduced particularly for the diameters $<$12 mm. Thermal efficiency or mean fluid outlet temperature is heavily dependent on the temperature distribution in the DARS, which owes largely to the rate at which radiation is absorbed per unit depth, rate of radiation extinction. Among other parameters such as the spatial distribution of nanoparticles and their opacity, the optical thickness is a function of length. As such DARS with larger diameters have increased optical thicknesses, thus the distance traversed in the medium by the incident radiation is increased. Due to this, there may be large regions within the fluid where the fluid temperature exhibited is invariant to that of the fluid inlet temperature as the radiant flux does not reach there and if so the magnitude is very low, as much of it has been absorbed by the outer fluid layers. The same effect is replicated if the volume fraction is too high, in this instance a surface-based absorber can be resembled whereby most of the incident radiation is absorbed by the outer layers, leaving a large region within the DARS with an invariant temperature. Conversely, if the particle concentration is too low, then optical efficiency suffers as the optical thickness of the medium is severely reduced this manifests reduced system yield as all of the radiant flux is not captured. Clearly, the volume fraction and DARS diameter must be optimized to achieve a maximum mean nanofluid outlet temperature or thermal efficiency. The DARS system was simulated with the two nanofluids and, in both cases, the minimum fluid outlet temperature of 250°C (523.15 K) was surpassed in a 5 mm diameter and 56.84 m long receiver tube.

Evidently, reducing the DARS receiver diameter reduces the mass flow rate of the circulating fluid and as such system output. Due to this, it is necessary to ascertain the effect of fluid flow velocity upon the mean fluid outlet temperature. In the simulations performed, fluid flow velocity has been varied from 0.002 to 0.0125 m s^{-1} corresponding to mass flow rates in the range between 0.0000416 and 0.000260 kg s^{-1}.

Table 2 conveys that in range of fluid velocities modeled, the DARS mean outlet temperature remains largely unaffected by variation in the fluid flow velocity. This is apparent as there is a nominal decrease of 5 K resulting from a significant increase, by a factor of 6.25, in the mass flow rate. Decrease in temperature depicted as fluid flow velocity is increased is expected due to the working fluid having a reduced exposure to incident solar irradiance, as the fluid traverses the receiver at an accelerated rate; aside from this the influence of fluid flow velocity, however, is minimal.

In view of the results achieved, it is apparent that graphene dispersed in Therminol VP-1 at a volume fraction of the 0.02% and aluminum dispersed in Therminol VP-1 at a volume fraction of 0.09% are the optimum configurations providing the DARS diameter is 5 mm; when the diameter surpasses 5 mm the mean fluid outlet temperature delivered is drastically reduced. Characteristically, it can further be seen that as the DARS diameter is increased the nanofluid with aluminum particles dispersed at a volume fraction of 0.002% is favorable as the working fluid yielding marginally higher temperatures, this is apparent upon examination of Figure 3. This is attributed to the change in optical thickness associated with increasing the DARS diameter, as a result, aluminum nanoparticles dispersed at 0.02% yield a more favorable optical response as radiation absorption and scattering occurs more uniformly across the medium due to reduced extinction coefficients. This heavily reinforces the rationale that nanofluids must be synthesized with astringent precedence being placed upon the optical response of the nanofluid relative to the geometric constraints of the DARS.

Table 2. *Variation of mean fluid outlet temperature (K) with fluid flow velocity.*

Fluid flow velocity (m s^{-1})	Mass flow rate (kg s^{-1})	Graphene nanofluid (K)	Aluminum nanofluid (K)
0.002	0.0000416	543.275	542.689
0.0075	0.000156	540.661	540.096
0.01	0.000208	539.498	538.941
0.0125	0.000260	538.345	537.801

4 CONCLUSION

When synthesizing heat transfer fluids for the purpose of implementation within direct absorption solar thermal energy systems, it is essential that nanomaterials are dispersed uniformly in the base fluid layer to enhance solar-weighted absorption and increase the potential yield from the system. Graphene was found to be a better absorber of solar radiation than aluminum; however, this does not warrant the use of graphene over aluminum as the material to be dispersed.

Nanofluid properties such as the volume fraction can be tailored relative to the solar absorption capability of the dispersed nanomaterial and the diameter of the DARS within which they are implemented to achieve maximum yield, ensuring that all of

the solar radiant energy is captured, and that there is a favorable fluid temperature distribution within the DARS owed largely to the radiant intensity attenuation rate. Suitability of one nanofluid over another thus comes down to economic viability and thermo-physical property enhancements that can be achieved via dispersion of the given nanomaterial as opposed to the rate of energy absorption in the medium and absorption capability of nanomaterials.

Economic viability is heavily dependent upon capital costs that will be incurred. In particular, graphene nanoparticles will incur heightened costs relative to aluminum nanoparticles and in view of the results presented for negligible gain. Additionally, further emphasis should be placed upon the longevity of the material in the suspension as this holds bearing over the level of variable costs in the form of maintenance required to relieve blockages or replace damaged or compromised components due to abrasion as a result of settled particulates.

Thermo-physical property enhancements could prove to be invaluable to achieve temperature uniformity within DARS due to enhanced thermal conduction or improve heat exchange efficiency downstream due to enhanced thermal conduction from nanofluids, providing grounds to assess the thermal performance of the nanofluid empirically. Reducing DARS diameter is favorable when trying to achieve higher mean fluid outlet temperatures. A smaller DARS diameter corresponds to a robust, compact concentrator structure allowing its implementation on existing industrial and commercial buildings or structures for harnessing solar energy in the form of heat, which is not possible with the existing designs of PTCs. A further significant increase in the nanofluid outlet temperature is expected if the DARS diameter is lowered <5 mm although the following would necessitate an increase in the fluid flow velocity to achieve higher flow rates for an improved performance, and perhaps augmentation of the volume fraction to optimize the optical response.

Fluid flow velocity has no appreciable effect upon the system yield in the range of velocities modeled; however, further work shall endeavor to extend the analysis to find the limiting velocity beyond which the system yield is significantly reduced. Further work has also been undertaken to optimize the thermo-fluidic-geometric parameters of the DARS to achieve an intended outlet temperature for a given concentrator.

REFERENCES

[1] Lei D, Wang Z, Li J. The calculation and analysis of glass-to-metal sealing stress in solar absorber tube. *Renew Energy* 2010;**35**:405–11.

[2] Medium Temperature Collectors. *IEA SHC – TASK 33 IEA SolarPACES – TASK IV Solar Heat for Industrial Processes.* http://www.iea-ship.org/documents/Medium_Temperature_Collectors_Task33-IV_email.pdf (7 October 2011, date last accessed).

[3] Abdelrahman M, Fumeaux P, Suter P. Study of solid-gas-suspensions used for direct absorption of concentrated solar radiation. *Sol Energy* 1979;**22**:45–8.

[4] Singh H, Eames PC. Correlations for natural convective heat exchange in CPC solar collector cavities determined from experimental measurements. *Sol Energy* 2012;**86**:2443–57.

[5] Incropera FP, De Witt DP. *Fundamentals of Heat and Mass Transfer*. Wiley, 1990.

[6] Solutia, 2013. *Therminol VP-1-Synthetic heat transfer fluid designed to meet the demanding requirements of vapour phase systems*. [Online] <http://www.therminol.com/pages/products/eu/vp-1.asp> (17 February 2013, date last accessed).

[7] Pop E, Varshney V, Roy AK. Thermal properties of graphene: fundamentals and applications. *MRS Bull* 2012;**37**:1273–81.

[8] Khullar V, Tyagi H, Phelan PE, *et al.*. Solar energy harvesting using nanofluids-based concentrating solar collector. *ASME J Nanotech Eng Med* 2012;**3**:031003.

[9] Yu W, Choi SUS. The role of interfacial layers in the enhanced thermal conductivity of nanofluids: a renovated Maxwell model. *J Nanopart Res* 2003;**5**:167–71.

[10] Leong KC, Yang C, Murshed SMS. A model for the thermal conductivity of nanofluids – the effect of the interfacial layer. *J Nanopart Res* 2006;**8**:245–54.

[11] Gueymard C. Parameterized transmittance model for direct beam and circumsolar spectral irradiance. *Sol Energy* 2001;**71**:325–46.

[12] Gueymard C. SMARTS, a simple model of the atmospheric radiative transfer of sunshine: algorithms and performance assessment. *Professional Paper FSEC-PF-270–95*, 1995. Florida Solar Energy Center.

[13] Tyagi H, Phelan P, Taylor RA. Predicted efficiency of a low-temperature nanofluid-based direct absorption solar collector. *ASME J Sol Eng* 2009;**131**:0410041–047.

[14] Taylor RA, Phelan PE, Otanicar TP, *et al.* Nanofluid optical property characterization: towards efficient direct absorption solar collectors. *Nanoscale Res Lett* 2011;**6**:2251–61.

[15] Otanicar TP, Phelan PE, Golden JS. Optical properties of liquids for direct absorption solar thermal energy systems. *Sol Energy* 2009;**83**:969–77.

[16] Bohren CF, Huffman DR. *Absorption and Scattering of Light by Small Particles*. Wiley, 1983.